A Semi-Empirical Backscattering Model at L-band and C-band for a Soybean Canopy with Soil Moisture Inversion

Roger D. De Roo, Yang Du, Fawwaz T. Ulaby
and M. Craig Dobson

Abstract

Radar backscatter measurements of a pair of adjacent soybean fields at L-band and C-band are reported. These measurements, which are fully polarimetric, took place over the entire growing season of 1996. To reduce the data acquisition burden, these measurements were restricted to 45° in elevation and to 45° in azimuth with respect to the row direction. Using the first order radiative transfer solution as a form for the model of the data, four parameters were extracted from the data for each frequency/polarization channel to provide a least squares fit to the model. For inversion, particular channel combinations were regressed against the soil moisture and area density of vegetation water mass. Using L-band cross-polarization and VV-polarization, the vegetation water mass can be regressed with an $R^2 = 0.867$ and a root-mean-square error of 0.0678 kg/m^2. Similarly, while a number of channels, or combinations of channels, can be used to invert for soil moisture, the best combination observed, namely, L-band VV-polarization, C-band HV- and VV-polarizations, can achieve a regression coefficient of $R^2 = 0.898$ and volumetric soil moisture root-mean-square error of 1.75%.

1 Introduction

For bare-soil surfaces, the backscattering coefficient, σ^0, is strongly dependent on the roughness and the moisture content of the soil surface layer [1, 2, 3].

Given two or more radar channels (such as simultaneous multi-polarization or multi-frequency observations), it is possible to estimate the volumetric moisture content, m_v, with good precision. Specifically, when multi-polarized L-band observations were used, the precision of the retrieved moisture was about 3.2% [3]. The data included observations made by a truck-mounted radar, by the JPL airborne AirSAR system, and by SIR-C.

This paper addresses the vegetation-covered case for a soybeans canopy. The first part describes the test site and data acquisition process. It is then followed with an analysis of the "direct problem", namely matching the measured data to a backscatter model. Then it ends with the development of a regression-based inversion algorithm (inverse problem) that predicts soil moisture content and vegetation biomass on the basis of multi-channel radar observations as input.

2 Experimental Measurements

The measurements reported in this study were conducted during the summer of 1996 at the Long-Term Ecological Research (LTER) site of the Kellogg Biological Station in Hickory Corners, Michigan. Three primary types of vegetation canopies were chosen for measurement: corn, which represents agricultural fields in which a stem or stalk is a dominant feature at microwave frequencies; soybeans and alfalfa, which represent agricultural fields that lack a dominant stem; and a field which had lain fallow for many years and is now populated with many native grasses. The present study will address the soybean observations only.

The radar backscatter measurements were made by a truck mounted radar system. All measurements were made at an incidence angle of 45° and at a range of 12-m in a fully polarimetric mode at both L-band (1.25 GHz) and C-band (5.4 GHz). Calibration accuracy is estimated at $\pm$ 0.5 dB for the copolarized backscattering coefficients, σ^0_{vv} and σ^0_{hh}, $\pm$ 1.0 dB for the cross-polarized backscattering coefficient, σ^0_{hv}, and $\pm 15°$ for phase difference between polarizations.

To reduce signal-fading variations of the backscattered signal, multiple measurements of the same target were performed under the same radar parameters (frequency, polarization and angle of incidence), but with a translation or rotation of the radar antennas. The figure of merit for the reduction of fading is the number of independent samples, which is the product of the

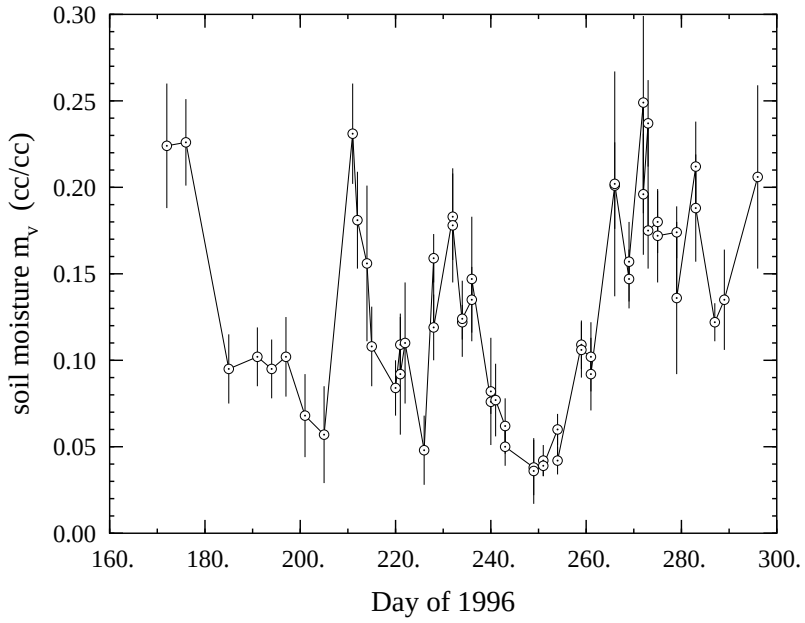

Figure 1: Variation of the soil moisture under the soybean canopy.

number of independent samples per spatial sample (due to frequency averaging) and the number of spatial samples measured. For each measurement reported in this study, the number of independent samples is 205 at L-band and 157 at C-band.

The radar measurements and associated canopy and soil observations were commenced on 20 June 1996 and were completed on 26 October. A total of 57 data sets were acquired, covering a wide range of conditions, extending from 0.02 kg/m^2 to 0.97 kg/m^2 in vegetation water mass, 3% to 26% in volumetric soil moisture, and 12 cm to 63 cm in canopy height. The variation of the moisture in the soybean fields measured in the growing season of 1996 is shown in Figure 1.

3 Backscatter Model

The Michigan Microwave Canopy Scattering (MIMICS) model was developed several years ago for predicting the backscatter from forest stands [4, 5]. We shall adopt the basic structure of the model for characterizing the backscatter

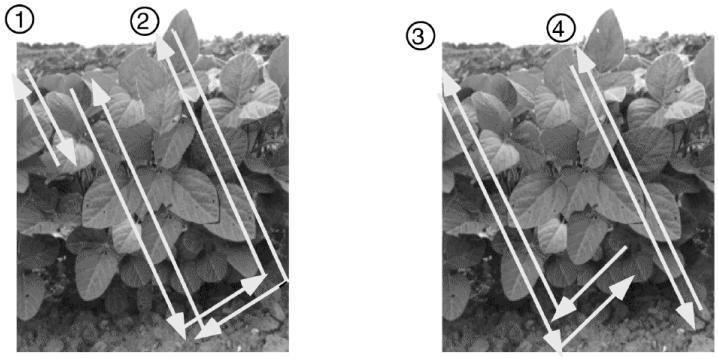

Figure 2: Scattering mechanisms considered in this paper for soybean canopies.

from soybeans, but we shall delete the scattering component associated with ground-trunk scattering because the architecture of a soybean plant does not have a vertical stalk. Hence, σ^0_{pq}, the pq-polarized backscattering coefficient (where p and q are each either v or h polarization) of the canopy may be expressed as:

$$\sigma^0_{pq} = \sigma^0_{pq_1} + \sigma^0_{pq_2} + \sigma^0_{pq_3} + \sigma^0_{pq_4}, \tag{1}$$

where each component represents a scattering mechanism, as illustrated in Fig. 1. For a particular pq-polarization configuration, these components are:

σ^0_1 = direct backscatter contribution from the canopy,

σ^0_2 = combined ground–canopy and canopy–ground forward scattering contribution,

σ^0_3 = ground–canopy–ground scattering contribution

σ^0_4 = direct backscatter contribution of the underlying soil surface (including two-way attenuation by the canopy).

The expressions for the four components are:

$$\sigma^0_{pq_1} = \frac{\sigma_{pq_1} \cos\theta}{\kappa_p + \kappa_q} \left(1 - T_p T_q\right), \tag{2}$$

$$\sigma^0_{pq_2} = 2T_pT_q(\Gamma_p + \Gamma_q)h\sigma_{pq_2} \tag{3}$$

$$\sigma^0_{pq_3} = \sigma^0_{pq_1}T_pT_q\Gamma_p\Gamma_q \tag{4}$$

$$\sigma^0_{pq_4} = \sigma^0_{pqs}T_pT_q, \tag{5}$$

where:

σ_{pq_1} = backscatter cross section per unit volume of the leaves and stems, (m^2/m^3),
σ_{pq_2} = bistatic cross section per unit volume of the leaves and stems, (m^2/m^3),
κ_p = p-polarized extinction coefficient of vegetation canopy, (Np/m),
T_p = p-polarized one-way transmissivity of the canopy,
$= e^{-\kappa_p h \sec\theta}$,
h = canopy height, m
Γ_p = p-polarized reflectivity of ground surface,
$= \Gamma_{po}\exp\left[-(2ks\cos\theta)^2\right]$
Γ_{po} = Fresnel reflectivity of a specular surface,
k $= 2\pi/\lambda$,
s = rms height of ground surface, (m)
σ^0_{pqs} = backscattering coefficient of soil surface in the absence of vegetation cover.

3.1 Soil Surface Model

For the soil surface, we adopt the semi-empirical model developed by Oh *et al.*, which was first introduced in 1992 [1] and then improved in a later study in 1994 [2]. The soil backscattering coefficient is given by:

$$\sigma^0_{vvs} = \frac{g\cos^3\theta}{\sqrt{p}}[\Gamma_v(\theta) + \Gamma_h(\theta)] \tag{6}$$

$$\sigma^0_{hhs} = p\sigma^0_{vvs} \tag{7}$$

$$\sigma^0_{hvs} = q\sigma^0_{vvs} \tag{8}$$

where

$$p = \frac{\sigma^0_{hhs}}{\sigma^0_{vvs}} = \left[1 - \left(\frac{2\theta}{\pi}\right)^{(0.314/\Gamma_0)} \cdot \exp(-ks)\right]^2 \tag{9}$$

$$q = \frac{\sigma^0_{hvs}}{\sigma^0_{vvs}} = 0.25\sqrt{\Gamma_0}(0.1 + \sin^{0.9}\theta)[1 - e^{-(1.4-1.6\Gamma_0)ks}] \tag{10}$$

$$g = 0.7\left[1 - e^{-0.65(ks)^{1.8}}\right], \tag{11}$$

$$\Gamma_0 = \left|\frac{\sqrt{\epsilon_s} - 1}{\sqrt{\epsilon_s} + 1}\right|^2, \tag{12}$$

$$\Gamma_{ho}(\theta) = \left|\frac{\cos\theta - \sqrt{\epsilon_s - \sin^2\theta}}{\cos\theta + \sqrt{\epsilon_s - \sin^2\theta}}\right|^2 \quad , \tag{13}$$

$$\Gamma_{vo}(\theta) = \left|\frac{\epsilon_s\cos\theta - \sqrt{\epsilon_s - \sin^2\theta}}{\epsilon_s\cos\theta + \sqrt{\epsilon_s - \sin^2\theta}}\right|^2 \quad , \tag{14}$$

and ϵ_s is the relative complex dielectric constant of the soil:

$$\epsilon_s = \epsilon'_s - j\epsilon''_s. \tag{15}$$

The incidence angle θ is in radians and the models used for relating ϵ'_s and ϵ''_s to m_v, the volumetric soil moisture content, are given in Hallikainen *et al.*[6]. According to field tests, the soil was 51% sand and 13% clay.

The effect of soil surface roughness comes into the picture not only in terms of the direct soil backscatter component, $\sigma^0_{pq_4}$, but also in terms of forward scattering by the soil surface, $\sigma^0_{pq_2}$ and $\sigma^0_{pq_3}$; the p-polarized Fresnel surface reflectivity, Γ_{po}, is reduced by the exponential factor $[-(2ks\cos\theta)^2]$.

3.2 Vegetation Model

Next, we shall find the form of the functional dependence of the electromagnetic parameters of the vegetation, namely $\sigma_{pq_1}, \sigma_{pq_2}$, and κ_p, to the area density of vegetation water mass, m_w (kg/m^2). We start with the extinction coefficient κ_p. For a given canopy, we expect κ to be a function of (a) the canopy architecture, and (b) the dielectric constant, ϵ_v, of the vegetation

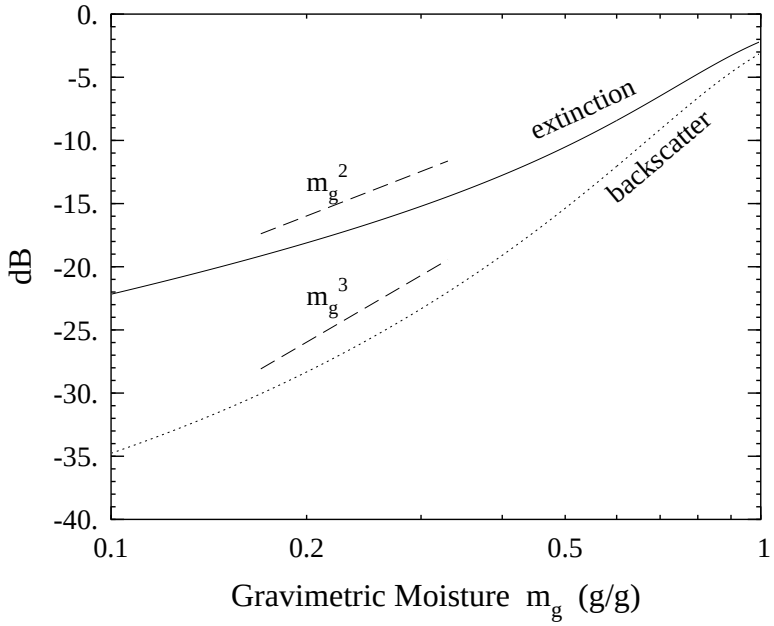

Figure 3: Dependence of the extinction and backscatter cross section of a single leaf upon its gravimetric moisture, after [7]. The vertical scale is normalized with respect to an equivalent perfectly conducting leaf of the same geometry. The extinction displays an approximately m_g^2 dependence while the backscatter displays an approximately m_g^3 dependence. The dashed line segments show perfect m_g^2 and m_g^3 dependence.

material. By canopy architecture, we mean the shapes, orientations, and sizes of the canopy constituents (defined relative to the wavelength λ), the incidence angle θ, and the wave polarization, p. Even though the extinction cross-section of an individual leaf or branch may exhibit a strong dependence on its orientation relative to the incident beam, we shall assume that the extinction coefficient κ_p– which is an ensemble average over the probability distribution characterizing the shapes, sizes, and orientations of leaves and branches– is independent of direction, which is a reasonable assumption for a canopy like soybeans. The dielectric constant of a vegetation material, ϵ_v, is strongly dependent on its moisture content. According to a study reported by Senior *et al.*[7], which included both a theoretical model and experimental verification, the extinction cross-section of a vegetation leaf (where first normalized to the extinction cross-section of a perfectly conductive leaf of the same size) varies approximately linearly with the gravimetric moisture m_g, when both quantities are expressed on a logarithmic scale. The gravimetric moisture m_g is the ratio of the mass of water in the leaf (wet weight - dry weight) to the total mass of the leaf (wet weight). Figure 3 is a reproduction of their results for the gravimetric moisture range between 0.1 and 0.9. The approximately linear response with a slope of approximately 2 (on a log-log scale) suggests that the extinction cross-section of a leaf may be expressed as:

$$\sigma^e = a_o m_g^2, \tag{16}$$

where a_o is a constant. Thus, for a canopy containing, on average, N leaves per m^3, the extinction coefficient becomes

$$\kappa_p = N a_o m_g^2 \quad (\mathrm{Np/m}). \tag{17}$$

The results of Senior *et al.* also suggest that the backscatter is proportional m_g^3. But these conclusions are valid only for the restrictive case where the leaves are oriented to backscatter specularly from the surface of the leaves. For the more complicated and more realistic case of a broad distribution of orientations of leaves, and including stems, the MIMICS radiative transfer model [4, 5] was used to find the extinction and backscatter averaged over the shape, size and orientation distributions of the detailed soybean vegetation parameters as provided in [8, 9, 10]. The results of these calculations for L-band and C-bands are shown in Figures 4 and 5. It was found that for both

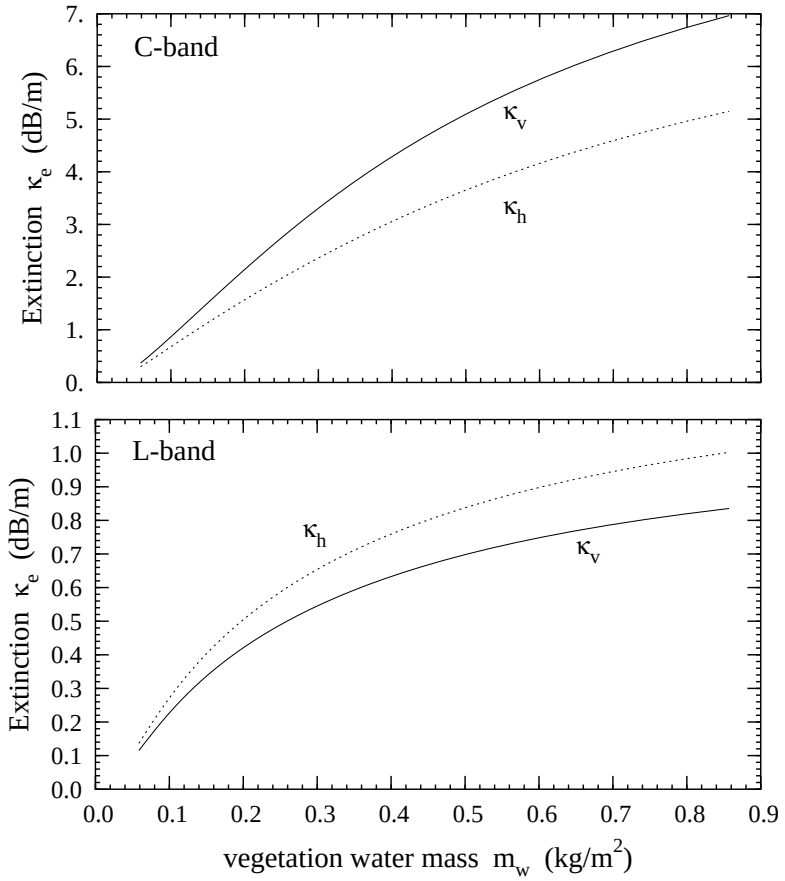

Figure 4: Dependence of the extinction on the area density of vegetation water mass in leaves and stems at C-band and L-band. Whereas the extinction exhibits a strong frequency dependence, all of the extinction rates are approximately proportional to $\sqrt{m_w}$.

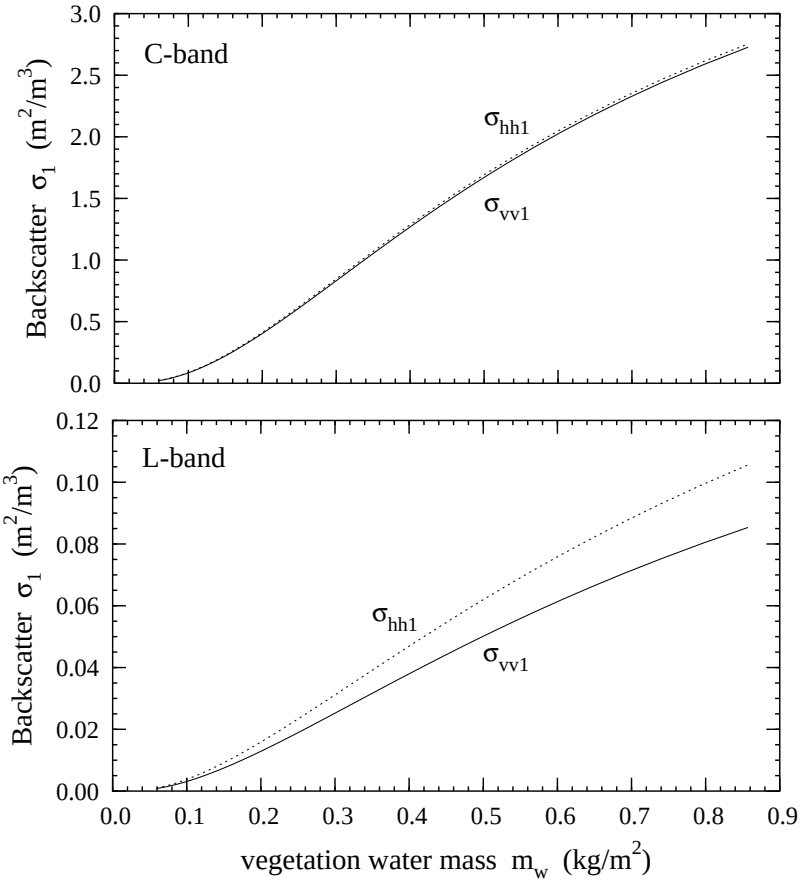

Figure 5: Dependence of the backscatter RCS per unit volume on the area density of vegetation water mass in leaves and stems at C-band and L-band. Both VV and HH exhibit a dependence which is roughly proportional to m_w.

VV and HH polarizations, the mean extinction was proportional to $\sqrt{m_w}$, where m_w is the area density of vegetation water mass in kg/m^2. The MIMICS model calculations for the mean backscatter, shown in Figure 5, exhibit a linear dependence on m_w. MIMICS model calculations for the backscatter and bistatic phase matrices indicate that this linear dependence on m_w is appropriate for both the backscatter and bistatic canopy scattering terms in the radiative transfer model.

The curves in Figures 4 can be described with more faithful but more complicated dependencies on m_w, such as $\ln m_w$ or $b_1\left(\frac{1-m_w/b_2}{1+m_w/b_2}\right)$. Nonetheless, the fact that the curves themselves are based on a vegetation model developed for forest canopies and that the formulas found here are used in the semi-empirical model below only to tie the dependence of the vegetation moisture to extinction and/or volume backscattering, these more complicated dependencies are not justified. Indeed, we have tried other formulations for the dependence of extinction and scattering on m_w, and the semi-empirical model goodness-of-fit values were either insignificantly different or somewhat worse than those reported below. Therefore, the extinction is assumed to be proportional to $\sqrt{m_w}$ and the scattering is proportional to m_w.

3.3 A semi-empirical forward scattering model

Combining the first order radiative transfer solution of eqn. (1) with the results of the study of the dependence of the scattering and extinction on the vegetation water mass, we obtain the following equation to which the data must be fit:

$$\sigma^0_{pq} = a_{\text{bias}}\left(\frac{\sigma_{pq_1}\cos\theta}{2\kappa_{pq}}\left(1-T^2_{pq}\right)\left(1+T^2_{pq}\Gamma_p\Gamma_q\right)+T^2_{pq}\left(2(\Gamma_p+\Gamma_q)h\sigma_{pq_2}+\sigma^0_{pqs}\right)\right) \tag{18}$$

where

$$\sigma_{pq_1} = a_2 m_w/h \tag{19}$$

$$\sigma_{pq_2} = a_3 m_w/h \tag{20}$$

$$\kappa_{pq} = a_4\sqrt{m_w/h} \tag{21}$$

$$T_{pq} = e^{-\kappa_{pq}h\sec\theta} \tag{22}$$

and the remaining symbols ($h, \theta, \Gamma_p, \Gamma_q, \sigma^0_{pqs}$) retain their definitions from the previous section. The units of a_2 and a_3 are in RCS per kilogram of vegetation

moisture, and a_4 is in Nepers per root kilogram of vegetation moisture per root meter of canopy height.

With the form of the scattering equation known, and a set of parameters either known (θ, λ, p, q) or measured $(\sigma^0_{pq}, h, m_w, m_g, m_v)$, the task of obtaining a semi-empirical forward scattering model becomes that of finding the unknown parameters $(a_{\text{bias}}, a_2, a_3, a_4, s)$ keeping in mind the fixed relationships between some of these parameters. The measured parameters, radar backscatter and soil moisture, are combined with interpolated values for the vegetation parameters (water mass, height and leaf gravimetric moisture) and inserted into a program which searches for the least squares error between the predicted backscatter and the measured backscatter, by varying the free parameters over their valid range in discrete steps. When a close fit is found, a Levenberg-Marquardt algorithm [11] is implemented which finds a local minimum of the error with respect to all the free parameters at once. The set of free parameters which provides the global minimum to the error is chosen as the set of free parameters most likely to represent the scattering mechanisms observed. This process is done independently for each frequency and polarization pair.

To determine the rms surface height of the soil, our radar measurements were divided into two sets. The first set consists of two days of polarimetric measurements made early in the season, before substantial biomass accumulated on the plants. The semi-empirical soil surface scattering model of Oh *et al.* [2] was used on the C-band measurements of this set to invert the soil roughness, and a value of $s = 2.8$ cm was obtained. The L-band measurements lead to a similar roughness value. This is a mid-range value for the data used by Oh *et al.*, and is consistent with our photographic record. The remaining measurements, excluding those made after harvest, constitute the second set, and were used for finding the forward and inverse models described below.

For C-band, the normalized roughness value of $ks = 3.2$ indicates that the reflection from the ground at this frequency would be insignificantly small. Nonetheless, the Levenberg-Marquardt algorithm attempts to find a best fit of the model to the data and reports that the bistatic scattering in the canopy is on the order of 50 dB in excess of the backscattering in the canopy. This numerical compensation for the large ks value is physically inappropriate, and so for C-band we have forced σ_{pq2} to be equal to σ_{pq1} (that is, $a_3 = a_2$). At L-band, however, the normalized roughness is much more modest at $ks = 0.74$, and all the parameters have been allowed to vary

Freq	Pol	a_2	a_3	a_4	bias	rms error	max error	P
		m^2/kg	m^2/kg	$Np/(kg/m)^{1/2}$	dB	dB	dB	%
C	HH	0.151	$= a_2$	0.341	2.50	0.71	1.79	23
C	VV	0.170	$= a_2$	0.484	3.47	0.73	1.82	16
C	HV	0.051	$= a_2$	0.948	5.16	0.55	1.26	84
L	HH	0.0	0.132	0.126	3.39	0.81	1.38	1.5
L	VV	0.0025	0.0605	0.0	4.78	0.62	1.81	49
L	HV	0.0	0.0351	0.125	5.06	0.70	1.95	15

Table 1: Best fit free parameters for semi-empirical soybean model.

independently for the minimization algorithm.

We have included in equation (18) a bias factor, a_{bias}, because, without it, the data could not be accurately described by the model. The usual suspects, namely calibration and measurement errors, have been investigated, but we have not located any source of error. It is possible that the semi-empirical soil surface scattering model of Oh *et al.*, developed for bare soils, may not be directly applicable to a surface under a growing crop. Also, rain may significantly alter the soil roughness over the course of the growing season. For any of these reasons, the bias value may not be appropriate for other data sets. Nonetheless, the existence of an arbitrary but constant bias does not alter the objectives or the conclusions of this paper.

The free parameters that were found to provide the best fit for the set of soybean measurements are shown in Table 1. The rms error and maximum error are given in dB. The goodness-of-fit measure P represents the statistical level required to reject the model, or, in other words, the probability that a repetition of the measurements would result in a worse fit to the model, assuming that this model and the values of these parameters are correct. The measure P takes into account the known or assumed errors in the measurements, while the rms error or maximum error measures do not. Values of P greater than approximately 5% indicate that a more complicated model is unlikely to provide a better fit to the data. The low value of P for L-band HH indicates that the model is not a very good representation of the observations. The reason the fit for L-band VV-polarization is better than HH may be due to the fact the numerical fitting algorithm has a better chance of finding a good fit for some values of the free parameters for VV. This is because Γ_v, the V-polarized ground reflectivity, has a larger dynamic

range due to the variation in soil moisture, m_v, than does Γ_h.

While the free parameters for each polarization and frequency are derived independently of each other, certain known relationships exist between them. The extinction parameter, a_4, while not independent of polarization, should be only weakly sensitive to polarization, but should be much higher for C-band than for L-band. The canopy scattering terms, a_2 and a_3, should also be much higher for C-band than L-band. Within a given frequency and polarization, it is expected that the bistatic scattering from the canopy would be stronger than backscattering, and so $a_3 > a_2$. While we have essentially turned off the bistatic term at C-band because of the rough ground, at L-band the bistatic term so dominates the backscatter that the best fit parameters for backscatter are zero for two polarizations. Otherwise, all of these expectations are realized in the values of the free parameters derived.

An analysis of the contributions from the mechanisms described in Figure 2 for the mature soybean canopy show that the ground-canopy-ground scattering interaction described by σ^0_{pq3} in equation (4) is negligible for all polarizations and both frequencies investigated. From the parameters for C-band VV and HH backscatter in Table 1, the direct ground backscatter, as attenuated by the canopy, is comparable to the crown backscatter, the only other significant contribution. This somewhat surprising result that the direct ground may contribute so much may be a consequence of the fact that on the particular fields measured the row spacing was 30 inches, which, coupled with the dry summer, resulted in a canopy with significant discontinuities. For C-band HV polarization, the direct backscatter from the crown dominates.

The predicted dominant scattering mechanism is polarization dependent at L-band. For VV polarization, zero attenuation provided the best fit to the observations, and as a result the direct backscatter from the ground dominates the terms from the canopy. For HH polarization, the direct ground and crown–ground terms are comparable, while for HV the crown–ground interaction term is most important. For both HH and HV at L-band, the algorithm estimated no direct crown backscatter contribution, but considering the relative strengths of the direct crown and crown–ground terms for VV polarization, it is not too surprising that the algorithm could not accurately quantify the weaker mechanism from the data. Similarly, the weak extinction at L-band results in a best fit prediction of no extinction for VV polarization.

Ulaby and Wilson [12] report direct measurements of attenuation through a soybean crop at L-band and C-band. In addition to measurements of a full

Freq	Pol	measured	predicted
C	H	3.1 ± 0.5 dB	2.3 dB
L	H	0.7 ± 0.4 dB	0.85 dB
C	V	9.9 ± 1.6 dB	3.3 dB
L	V	2.6 ± 0.5 dB	0 dB

Table 2: Comparison of measurements by Ulaby and Wilson [12] and equation (21) for one-way extinction through a full soybean canopy.

soybean canopy at an incidence angle of 52° and perpendicular to the rows, they also defoliated the plants and repeated the measurement, to determine the relative contributions to extinction due to leaves and stems. Table 2 shows their measurements for the one way full canopy losses, with the results of applying equation (21) to the ground truth reported in their paper for comparison. The H-polarized predictions compare very favorably with their measurements. Their measurements for V-polarization are higher, while our model falls short of these observations. Their defoliation experiments lead to a conclusion that the stems dominate the V-polarized extinction but only contribute about 50% of the H-polarized extinction at L- and C-bands. Our largest measured water mass density in the stems is one fourth of theirs. Thus, while our derived H-polarized extinction appears to extrapolate nicely to a healthy canopy, the same cannot be said for our V-polarized extinction expressions.

Comparisons of the semi-empirical model calculations with the measured data are shown Figures 6 and 7.

4 Inversions

The objective of the exercise is not to simply understand how the backscattering from a crop such as soybeans depends on scientifically and commercially important quantities like soil moisture and biomass, but to use the measurements of backscatter to determine estimates of these important quantities. This section outlines the approaches used to invert the semi-empirical model developed in the previous section.

As a first step, the desired invertible quantities, namely soil moisture and vegetation water mass, are regressed against the six radar channels (L-band

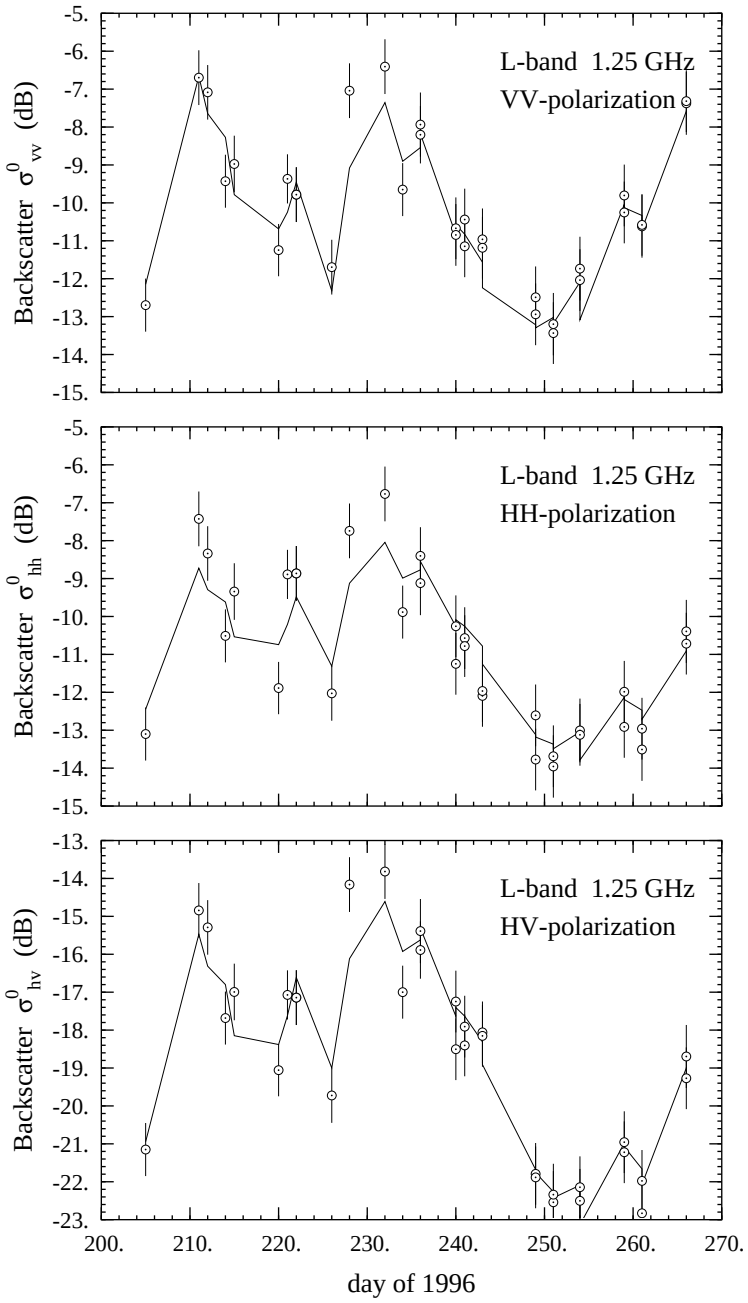

Figure 6: Comparison of the semi-empirical model to the measured data at L-band. The angle of incidence is fixed at 45° and the look direction relative to the row direction was also fixed at 45°.

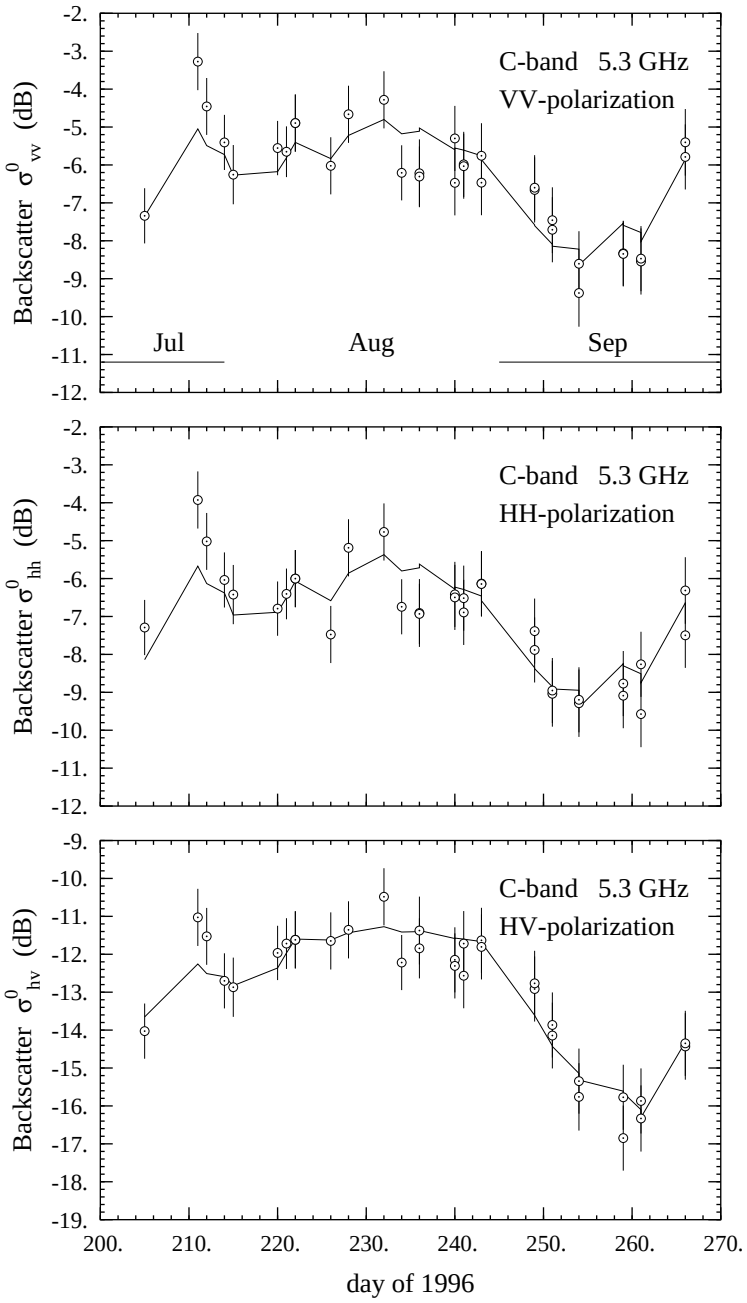

Figure 7: Comparison of the semi-empirical model to the measured data at C-band. The angle of incidence is fixed at 45° and the look direction relative to the row direction was also fixed at 45°.

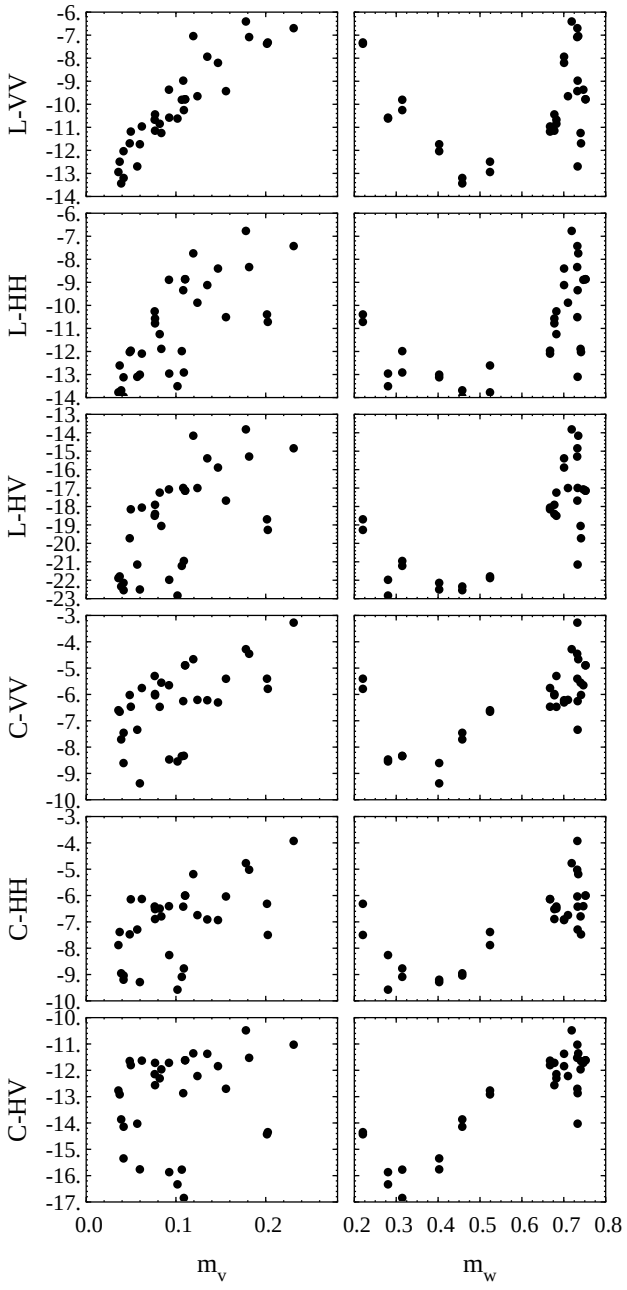

Figure 8: Visual results of the regression of the measured soil moisture m_v, left column, the area density of the vegetation water mass m_w, right column, and the six radar channels. Only L-band VV shows a strong direct correlation with m_v.

and C-band, each with VV, HH, and HV), as shown graphically in Figure 8. The fifteen combinations of ratios of those radar channels were similarly regressed against m_v and m_w. The vast majority of these regressions show very poor correlation between the radar quantity and the desired parameter, but a few show modest correlations. The single channel with the best correlation with soil moisture is, not surprisingly, L-band VV polarization, since the relatively long wavelength permits substantial penetration of the canopy and the vertically polarized Fresnel reflection coefficient of the surface is sensitive to soil moisture. For all polarizations, L-band has a much higher dynamic range than C-band, and much larger measurement to measurement variation. For the three L-band polarizations, VV is most faithfully described by the forward model.

The channel ratio with the best correlation to soil moisture is the L-band cross-pol to C-band cross-pol ratio. The L-band cross-pol data has a slightly larger dynamic range than does either co-pol, and the C-band cross-pol has the smallest sensitivity of all channels measured to soil moisture. This particular combination provides the large dynamic range of the L-band measurements to soil moisture with a correction for vegetation water mass provided by the C-band channel.

The channel ratio with the best correlation to vegetation water mass is L-band cross-pol to L-band VV-polarization. The best fits to our measured data, together with the root-mean-squared error and the regression coefficients, for each of these physical quantities are given by

$$\frac{\sigma^0_{L-HV}}{\sigma^0_{C-HV}} = 1.9360 m_v^{0.8237} \qquad \text{rmse} = 3.25\% \qquad R^2 = 0.633 \quad (23)$$

$$\frac{\sigma^0_{L-HV}}{\sigma^0_{L-VV}} = 0.2510 m_w^{1.0277} \qquad \text{rmse} = 0.0678 \text{ kg/m}^2 \qquad R^2 = 0.867 \quad (24)$$

In these equations, σ^0 is given in RCS per unit area (m^2/m^2). Figures 9 and 10 show the resultant inversion of our measured data for the soil moisture and vegetation water mass. Ferrazzoli *et al.* [13] have also found that L-band cross-pol to be an important predictor of vegetation biomass for crops.

While the regression for vegetation water mass in (24) is quite good, the use of (23) for inversion is less than ideal. The single channel with the highest sensitivity to soil moisture is the L-band VV-polarization, as is evident from Figures 6 and 7. The following equations show the linear regression of this channel, together with two combinations of channel ratios which improve the

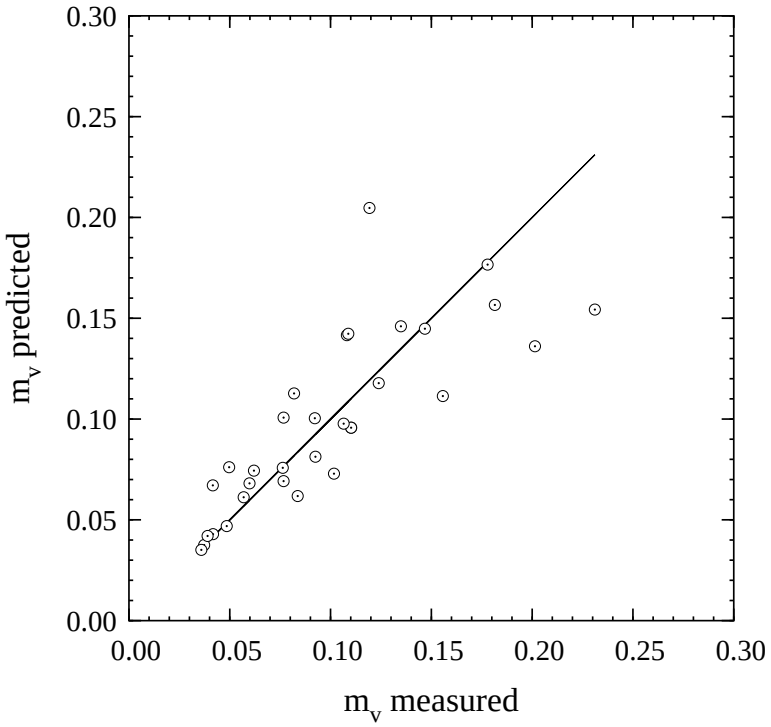

Figure 9: Comparison of the measured soil moisture with inverted soil moisture derived from both L-band and C-band cross-polarization radar measurements.

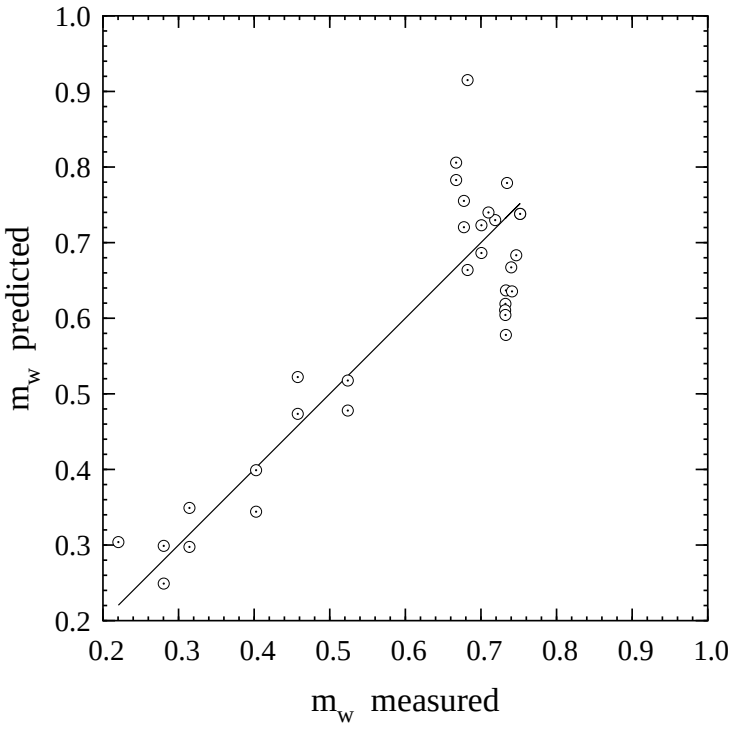

Figure 10: Comparison of the measured vegetation water mass with inverted vegetation water mass derived from both L-band VV- and cross-polarization radar measurements.

correlation significantly.

$$m_v = 0.3489 + 0.0244\sigma^0_{L-VV} \qquad \text{rmse} = 2.13\% \qquad R^2 = 0.842 \quad (25)$$

$$m_v = 0.2338 + 0.0244\sigma^0_{L-VV} - 0.0142\left(\sigma^0_{C-HV} - \sigma^0_{C-VV}\right) \qquad \text{rmse} = 1.75\% \qquad R^2 = 0.898 \quad (26)$$

$$m_v = 0.2483 + 0.0272\sigma^0_{L-VV} - 0.0139\left(\sigma^0_{C-HV} - \sigma^0_{C-VV}\right) - 0.0063\left(\sigma^0_{L-HV} - \sigma^0_{C-HV}\right) \qquad \text{rmse} = 1.72\% \qquad R^2 = 0.904 \quad (27)$$

In these equations, σ^0 is given in dB.

Use of L-band VV-polarization alone is an improvement over the exclusive use of the L-band to C-band cross-pol ratio, but it is improved with the inclusion of the C-band cross-to-co-pol ratio, which is essentially a correction for the dependence of L-band VV on the vegetation water mass. Further inclusion of L-band to C-band cross-pol ratio provides negligible improvement in the correlation. Figure 11 shows the improved inversion of our measured data for the soil moisture using equation (26).

5 Conclusions

A series of measurements of the radar backscatter from soybeans is reported. The soybeans fields were located at the Kellogg Biological Station in Hickory Corners, MI, USA. The series of 57 measurements on these fields commenced on 20 June 1996 and were completed on 26 October 1996. Each measurement was fully polarimetric at both L-band and C-band, made at an incidence angle of 45° and also at 45° with respect to the crop row structure, and contains a minimum of 157 independent samples. With each measurement is a set of soil core samples used to determine the volumetric soil moisture; several destructive samples over the growing season were used to obtain measures of the above-ground biomass, including the area density of vegetation water mass. Measurements from the center of this period, when the soybean biomass was not negligible, were used to create a semi-empirical forward scattering model. This forward scattering model is based on the first-order radiative transfer solution, akin to MIMICS, used for the prediction of forest backscatter. Four parameters are determined from the data: two for scattering from the leaves and one for extinction through the canopy, and one for the rough ground. Another parameter for describing the rough ground

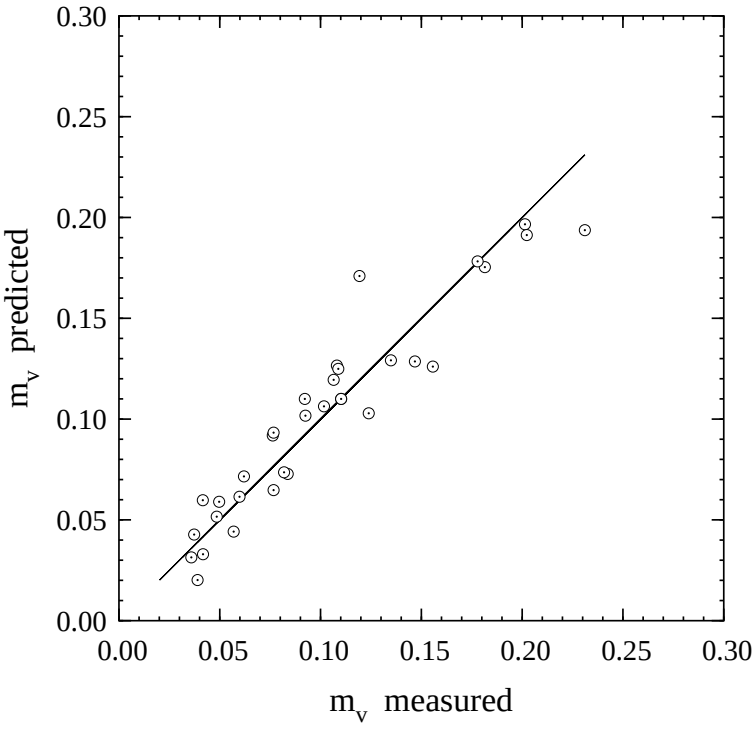

Figure 11: Comparison of the measured soil moisture with inverted soil moisture derived from radar measurements using equation (26).

backscatter, the effective rms surface height, was independently determined from radar measurements early in the growing season; these measurements are not included in the dataset used to fit the radiative transfer model. A slightly modified semi-empirical model proposed by Oh *et al.* [2] is used for direct backscatter from the ground in the forward scattering model. The four parameters are determined independently for each frequency and polarization; very good fits to the model are achieved for all polarizations at C-band and for VV-polarization at L-band.

Subsets of the measured data in frequency and polarization are used to obtain inversion models. For a measure of the biomass, a combination of L-band VV-polarization and HV-polarization was found to have the highest correlation to the area density of vegetation water mass, with a regression coefficient $R^2 = 0.867$ and a root-mean-square error of 0.0678 kg/m^2. Numerous polarizations and frequencies, singly or in combination, can be used to invert for soil moisture. The use of cross-polarized backscattering at both L-band and C-band for soil moisture inversion, first reported here, provides an adequate measure for the soil moisture. L-band VV-polarized backscatter, however, is the single channel with the largest dynamic range due to soil moisture changes and simultaneously well-described by the forward scattering model. Its use, in conjunction with the C-band cross- to co-polarized ratio as a correction for biomass effects, yields a regression against volumetric soil moisture with root-mean-square error of 1.75% and a regression coefficient of $R^2 = 0.898$.

Acknowledgments

The authors wish to express their sincere gratitude to Dr. Sandra Halstead and Dr. Phil Robertson of the Kellogg Biological Station for the use of the NSF Long Term Ecological Research site and assistance provided throughout the project. Thanks are also due to Dr. Tsen-Chieh Chiu, Prof. Kamal Sarabandi, Yanni A. Kouskoulas and Daniel J. Zahn for their guidance and assistance in various stages of this project. Last, but not least, the authors wish to thank Isaac D. Fehrenback, C. N. Peter Shum, H. S. Grace Tong, Sucila N. Fernandes, James H. Buck and Larina A. Robbins for their invaluable assistance in the acquisition of the data presented in this paper.

References

[1] Y. Oh, K. Sarabandi, and F. T. Ulaby, "An empirical model and an inversion technique for radar scattering from bare soil surfaces," *IEEE Transactions on Geoscience and Remote Sensing*, vol. 30, no. 2, pp. 370–381, March 1992.

[2] Y. Oh, K. Sarabandi, and F. T. Ulaby, "An inversion algorithm for retrieving soil moisture and surface roughness from polarimetric radar observation," in *Digest*, volume 3 of *IEEE International Geoscience and Remote Sensing Symposium (IGARSS '94)*, pp. 1582–1584, Pasadena, CA, 8–12 August 1994.

[3] F. T. Ulaby, P. C. Dubois, and J. van Zyl, "Radar mapping of surface soil moisture," *Journal of Hydrology*, vol. 184, pp. 57–84, 1996.

[4] K. C. McDonald, M. C. Dobson, and F. T. Ulaby, "Using MIMICS to model L-band multiangle and multitemporal backscatter from a walnut orchard," *IEEE Transactions on Geoscience and Remote Sensing*, vol. 28, no. 4, pp. 477–491, July 1990.

[5] F. T. Ulaby, K. Sarabandi, K. C. McDonald, M. Whitt, and M. C. Dobson, "Michigan Microwave Canopy Scattering Model," *International Journal of Remote Sensing*, vol. 11, no. 7, pp. 1223–1253, 1990.

[6] M. T. Hallikainen, F. T. Ulaby, M. C. Dobson, M. A. El-Rayes, and L. Wu, "Microwave dielectric behaviour of wet soil, Part I: Empircal models and experimental observations," *IEEE Transactions on Geoscience and Remote Sensing*, vol. 23, no. 1, pp. 25–34, January 1985.

[7] T. B. A. Senior, K. Sarabandi, and F. T. Ulaby, "Measuring and modeling the backscatter cross section of a leaf," *Radio Science*, vol. 22, no. 6, pp. 1109–1116, November 1987.

[8] T.-C. Chiu, *Electromagnetic Scattering from Rough Surfaces Covered With Short Branching Vegetation*, PhD dissertation, University of Michigan, Ann Arbor, 1998.

[9] J. J. Hanway and C. R. Weber, "Dry matter accumulation in soybean (*Glycine max* (l) Merrill) plants as influenced by N, P, and K fertilization," *Agronomy Journal*, vol. 63, pp. 263–266, March–April 1971.

[10] A. G. Norman, editor, *Soybean Physiology, Agronomy, and Utilization*, chapter 2, pp. 17–44, Academic Press, New York, 1978.

[11] W. H. Press, S. A. Teukolsky, W. T. Vetterling, and B. P. Flannery, *Numerical Recipes in Fortran: The Art of Scientific Computing*, University Press, Cambridge, second edition, 1992.

[12] F. T. Ulaby and E. A. Wilson, "Microwave attenuation properties of vegetation canopies," *IEEE Transactions on Geoscience and Remote Sensing*, vol. 23, no. 5, pp. 746–753, November 1985.

[13] P. Ferrazzoli, S. Paloscia, P. Pampaloni, G. Shiavon, S. Sigismondi, and D. Solimini, "The potential of multifrequency polarimetric SAR in assessing agricultural and arboreous biomass," *IEEE Transactions on Geoscience and Remote Sensing*, vol. 35, no. 1, pp. 5–17, January 1997.